LBL-38260
UC-600
Preprint

Lawrence Berkeley Laboratory
UNIVERSITY OF CALIFORNIA

EARTH SCIENCES DIVISION

Submitted to Water Resources Research

Flow and Tracer Transport of a Doublet Well System in an Aquifer with a Circular Inclusion

S.P. Pozdniakov, C.F. Tsang, and V.A. Korneev

January 1996

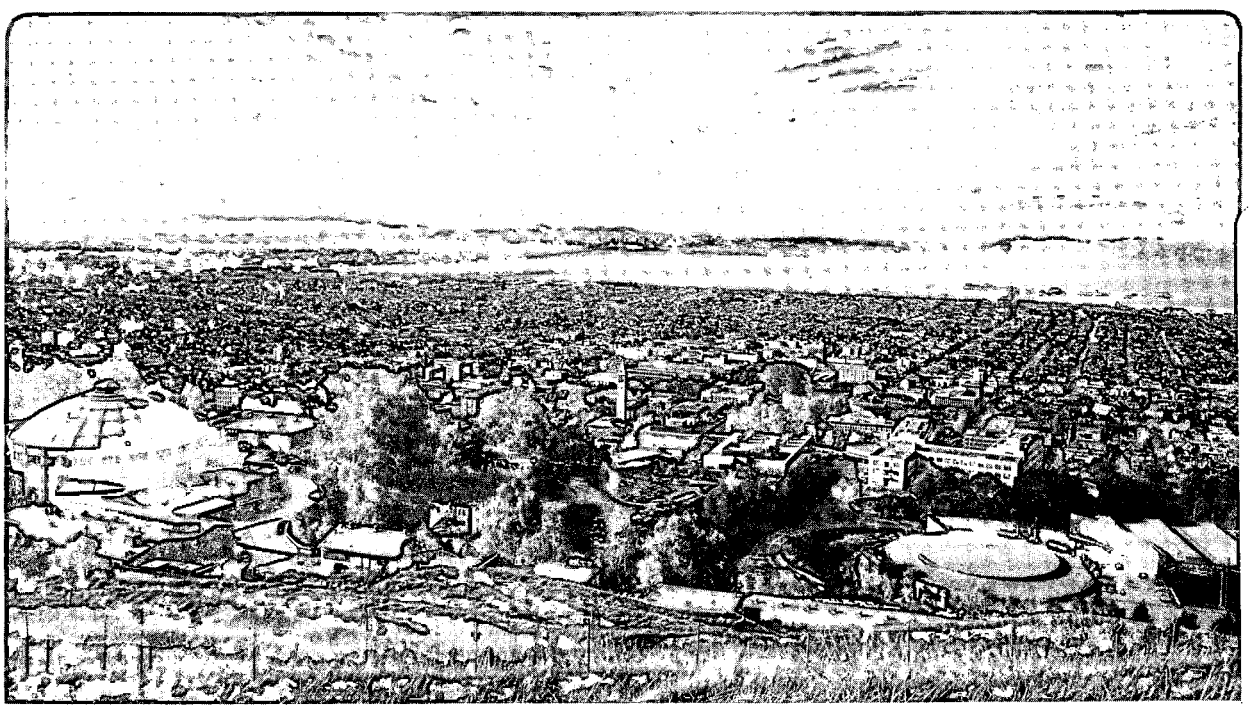

REFERENCE COPY
Does Not
Circulate
Bldg. 50 Library.
Copy 1
LBL-38260

Prepared for the U.S. Department of Energy under Contract Number DE-AC03-76SF00098

DISCLAIMER

This document was prepared as an account of work sponsored by the United States Government. While this document is believed to contain correct information, neither the United States Government nor any agency thereof, nor the Regents of the University of California, nor any of their employees, makes any warranty, express or implied, or assumes any legal responsibility for the accuracy, completeness, or usefulness of any information, apparatus, product, or process disclosed, or represents that its use would not infringe privately owned rights. Reference herein to any specific commercial product, process, or service by its trade name, trademark, manufacturer, or otherwise, does not necessarily constitute or imply its endorsement, recommendation, or favoring by the United States Government or any agency thereof, or the Regents of the University of California. The views and opinions of authors expressed herein do not necessarily state or reflect those of the United States Government or any agency thereof or the Regents of the University of California.

LBL-38260
UC-600

Submitted to Water Resources Research
November 1995

Flow and Tracer Transport of a Doublet Well System in an Aquifer with a Circular Inclusion

S.P. Pozdniakov, C.F. Tsang, and V.A. Korneev

Earth Sciences Division
Ernest Orlando Lawrence Berkeley National Laboratory
University of California
Berkeley, CA 94720

January 1996

This work was jointly supported by the Department of Energy, Office of Environmental Management, Office of Technology Development (D0E/EM-OTD), and the Department of Energy, Office of Energy Research, Office of Basic Energy Sciences (DOE/ER-BES), under Contract Number DE-AC03-76SF00098.

Submitted to WRR
November 1995.

Flow and Tracer Transport of a Doublet Well System in an Aquifer with a Circular Inclusion

S.P. Pozdniakov[†], Chin-Fu Tsang, and V.A. Korneev

Earth Sciences Division, Ernest Orlando Lawrence Berkeley National Laboratory, University of California, Berkeley, CA 94720

ABSTRACT

Steady state flow and tracer transport between an injection well and a pumping well in an aquifer with a circular inclusion are investigated using analytical and numerical techniques. A rigorous solution for the flow and velocity field was obtained. Calculations of transport are based on a particle-tracking technique on the advective field. Tracer breakthrough curves are calculated to study the influence of the location and hydraulic parameters of the circular inclusion. Examples are given to show the resulting impact on of the effective aquifer macroscopic parameters determined from an analysis of doublet flow and tracer tests without considering the presence of the inclusion.

INTRODUCTION

In the design of an optimal groundwater remediation strategy for contaminated heterogeneous aquifers, one needs to estimate *in situ* flow and transport parameters. One method for field-scale determination of transport parameters is a tracer injection test. There are two common test schemes: the radial convergent test with flow dominated by a single well and the doublet test with a divergent-convergent flow pattern based on two wells. The doublet test is considered to be more appropriate for a heterogeneous aquifer (*Mironenko and Rumynin*, 1986 and *Gelhar*, 1993).

[†] Current address: Department of Hydrogeology, Moscow State University, Vorobyovy (Lenin's) Hills, 119899, Moscow, Russia

Radial flow and transport in heterogeneous media have been investigated by many authors, including *Shvidler* (1964), *Desbarats* (1992), *Moreno and Tsang* (1991), *Vandenberg* (1977), and *Mironenko and Rumynin* (1986). Flow in a multiple-well system in heterogeneous media has been studied by *Gomez-Hernandez and Gorelick* (1989), *Desbarats* (1993), and others. Transport problems for such systems using advective and advective-dispersion approaches were studied by *Grove* (1971) and *Mironenko and Rumynin* (1986), who obtained analytical solutions for the advective-dispersive problem for a scale of heterogeneity much less than the doublet dimension, defined as the distance between injection and pumping wells. Numerical solution methods for this problem have been published by *Huyakorn et al.* (1986).

The advantages of the doublet-test scheme for the entire thickness of the aquifer have been discussed by *Mironenko and Rumynin* (1986). For equal injection and production flow rates, the flow lines of a doublet form a closed net between the two wells, thus effectively averaging the aquifer properties over the doublet's area of influence. It seems that this advantage exists only for the case where the doublet dimension is much larger than the scale of heterogeneity. In the work of *Tsang et al.* (1988), tracer transport in a statistically heterogeneous aquifer was studied, and it was shown that flow becomes channelized due to the influence of heterogeneity. Furthermore, for many fractured and porous aquifers the scale of heterogeneity of hydraulic conductivity or transmissivity can be tens of meters. On the other hand, from a practical point of view, the doublet dimension is usually less than two hundred meters. Hence, the case where the doublet dimension is the same order as the scale of heterogeneity is common. In the work of *Pozdniakov and Tsang* (1994), numerical transport modeling of a doublet system for a heterogeneous aquifer with the scale of heterogeneity similar to the doublet dimension was conducted. It showed that large differences in breakthrough curves were obtained for tests at different locations in the same heterogeneous aquifer. *Kurowski et al.* (1994) also studied the effects of aquifer heterogeneity on the doublet test for the special case of a confined circular aquifer.

The purpose of the present study is to investigate the influence of aquifer heterogeneity on the results of the tracer test in the simplest case of heterogeneity—a circular inclusion in an otherwise homogeneous aquifer. The choice of this model is explained by the possibility of obtaining an exact analytical solution for the flow problem. This model will be useful for estimating the hydraulic properties of an artificial circular underground barrier created by injection into a well, for testing numerical programs that solve the advective-dispersive transport problem, and for studying uncertainty ranges from analyses of doublet flow and transport tests.

FLOW TOWARD A WELL NEAR A CIRCULAR INCLUSION

In this section we outline a method of obtaining the general solution for the two-dimensional hydraulic head field of a source in an aquifer with a circular inclusion. The solution to this problem seems straightforward but we were unable to find it in the available literature. The well-known *Landau and Lifshitz* (1962) solutions of such problems deal with uniform far-field flow with a circular inclusion. *Strack* (1989) presented the solutions of limiting cases: the flow toward the well near a circular lake and a circular impermeable inclusion in a uniform far-field system. Butler and Liu (1993) obtained the analytical solution for transient flow toward a pumping well in an aquifer with a circular inclusion in the Laplace-tranform domain with a numerical inversion procedure.

Consider the configuration shown in Fig. 1. Both the Cartesian $\{x,y\}$ and cylindrical $\{r,\theta\}$ coordinate systems will be used jointly. Centered at the origin of the systems is a cylinder of radius $r = R$. Placed outside the cylinder, the source has the coordinates $x = R_0$ and $y = 0$, where $R_0 \geq$ R. The volume within this cylinder is labeled $v = 1$, while the volume outside is labeled $v = 2$. The aquifer properties inside and outside the cylinder in general will be different and are described by their values of transmissivity

$$T_v = const. \ (v = 1,2). \tag{1}$$

Imposing an initial hydraulic head at a point in the medium $v = 2$ in the absence of an inclusion in $v = 1$ results in a field given by the Dupuit-Thiem equation

$$U_o(x,y) = U^0 + \frac{Q}{2\pi T_2}\ln\frac{\rho}{\Omega}, \quad \rho = \sqrt{R_0^2+r^2-2R_0 r\cos\theta}, \tag{2}$$

where $U_o(x,y)$ is the hydraulic head at a point (x,y) with distance ρ from the source, U^o is the constant hydraulic head on the boundary at a distance Ω from source, and Q is the pumping rate at the source. The interaction of this field with the cylinder field gives rise to an additional field both inside and outside the cylinder, denoted by

$$U_v = U_v(x,y) \quad (v = 1,2). \tag{3}$$

The additional fields (3) as well as the initial field (2) must all satisfy the equation of steady-state ground water flow, i.e., Laplace equation

$$\Delta \cdot U_v = 0 \quad (v = 1,2). \tag{4}$$

Furthermore, taken together, the fields must satisfy the boundary conditions on the surface of the cylinder, i.e., the hydraulic head and the normal velocity should be continuous. Thus we require that, at $r=R$,

$$U_0 + U_2 = U_1 \quad \text{and} \quad T_1\frac{\partial U_1}{\partial r} = T_2\left(\frac{\partial U_0}{\partial r} + \frac{\partial U_2}{\partial r}\right). \tag{5}$$

We also require that the additional fields remain finite within the circle and its radial derivative tend to zero at large distances from the circle. This is a well-posed problem in that, given the initial field, the boundary conditions are sufficient to solve for the additional fields and thus arrive at a unique solution to the problem. The way to find this unique solution in terms of U_1 and U_2 is shown in Appendix A. Alternatively the solution can be obtained by using an extension of the circular theorem given by Golubeva (1966). The results for the case of the source point inside the inclusion can be similarly derived and they are also given in Appendix A.

The total field outside the inclusion U_{out} equals to $U_0 + U_2$, and the total field inside the inclusion U_{ins} equals to U_1. In a Cartesian coordinate system of the source $Y = y$, $X = x - R_0$, the equation for fields inside the inclusion has the form:

$$U_{ins} = U_0 - \frac{Q}{2\pi T_2}\frac{\chi-1}{\chi+1}\ln\frac{\sqrt{X^2+Y^2}}{R_0}, \quad \chi = \frac{T_1}{T_2} \tag{6}$$

Outside of the inclusion it has the form:

$$U_{out} = -\frac{Q}{2\pi T_2}\frac{\chi-1}{\chi+1}\ln\sqrt{\frac{(R_0-X-\beta R)^2}{(R_0-X)^2+Y^2}}, \quad \beta = \frac{R}{R_0}. \tag{6a}$$

Using these equations, the groundwater drawdown $S = U^0 - U$ can be calculated for any ratios of transmissivities and distances from the source to the inclusion. From a practical point of view, it is important to estimate the influence of an inclusion on the productivity of a pumping well. The equation is

$$S = \frac{Q}{2\pi T_2}\left(\ln\frac{\Omega}{r_w} + \xi\right) \quad \text{or} \quad S = \frac{Q}{2\pi T_2}\ln\frac{\Omega}{r_e}; \quad r_e = r_w\exp(-\xi), \tag{7}$$

where S is the drawdown of groundwater head, r_w is the radius of the borehole, r_e is the effective radius of the well, and ξ is the dimensionless additional hydraulic resistance or skin of the well.

It is easy to show that in the most important case, when the well is close to the inclusion, i.e., $Y = 0$, $X = r_w$, and $X + R = R_0$, the additional hydraulic resistance has the form

$$\xi = \frac{\chi-1}{\chi+1}\ln\frac{r_w}{R_0}. \tag{8}$$

For extreme cases, equation (8) means that the effective radius of the well equals to R_0 for highly conductive inclusion ($\chi=\infty$), and equals to r/R_0 for an impermeable inclusion (χ = o).

FLOW FIELD FOR A DOUBLET WELL SYSTEM

Let us consider the doublet well system presented in Fig. 2. Using the superposition of solutions for a source near an inclusion, the initial groundwater drawdown S at a point (x, y) in such a system can be represented in the form

$$S = \frac{Q}{4\pi T_2}\left(\ln\frac{(\frac{d}{2}+x)^2+y^2}{(\frac{d}{2}-x)^2+y^2} + S_i'+S_w'\right), \tag{9}$$

where Q is the withdrawal/injection rate at the well, T_2 is the transmissivity of the aquifer, d is the distance between the two wells, S_w' and S_i' are additional dimensionless drawdown due to the interactions of the well field and the circular inclusion; and x,y are the Cartesian coordinates with the origin at half the distance between the two wells. Here S is positive when the groundwater head is less than the initial head.

The form of equation for additional drawdown depends on whether the location of the point is inside or outside the inclusion. For a point inside the inclusion, eq. (9) has the form

$$S = \frac{Q}{2\pi T_2(\chi+1)}\left(\ln\frac{(\frac{d}{2}+x)^2+y^2}{(\frac{d}{2}-x)^2+y^2} + (\chi-1)\ln\frac{R_i}{R_w}\right), \tag{10}$$

where R_w is the distance between the pumping well and the center of the inclusion, and R_i is the distance between the injection well and the center of inclusion.

For a point outside the inclusion, the equation for the additional drawdown can be written as

$$S_i' + S_w' = \frac{\chi-1}{\chi+1}\left(\ln\frac{(x'-\beta_i R)^2+y'^2}{x'^2+y'^2} - \ln\frac{(x''-\beta_w R)^2+y''^2}{x''^2+y''^2}\right), \tag{11}$$

where

$$x' = (x-x_c)\cos\varphi_i + (y-y_c)\sin\varphi_i$$

$$y' = (y-y_c)\cos\varphi_i + (x-x_c)\sin\varphi_i \tag{11a}$$

$$\beta_i = \frac{R}{R_i} \quad \text{and} \quad \beta_w = \frac{R}{R_w},$$

where x_c and y_c are the coordinates of the center of the inclusion and φ_i is the angle of rotation from the system of coordinates with the origin in the inclusion and the well placed on the positive part of the x' axis (see Fig. 2).

Coordinates x'', y'' are calculated using eq. (11a) with angle ϕ_w. When the doublet dimension is much less than the distance to the inclusion, the model of the perfect dipole can be used for field calculations (see Appendix C).

NUMERICAL CALCULATION OF BREAKTHROUGH CURVES

It is difficult to use eqs. (9) through (11) to obtain closed analytical equations for flow streamlines for arbitrary values of the coordinates and the transmissivity of the inclusion. Therefore, to calculate streamlines and transport in the system, a particle tracking method is used. A large number of particles is placed regularly on a circle with a small radius R_{int} centered at the injection well. For each particle, the equation of motion can be written in the form

$$n\frac{dX_p}{dt} = V_x(X_p, Y_p) \quad \text{and} \quad n\frac{dY_p}{dt} = V_y(X_p, Y_p) \ , \tag{12}$$

where X_p, Y_p are the coordinates of the particle, n is the aquifer porosity, and V_x, V_y are the components of the field velocity. They are calculated analytically for every point using equations for velocity in the form

$$V_x = -\frac{T}{m}\frac{\partial S}{\partial x}, \ V_y = -\frac{T}{m}\frac{\partial S}{\partial y}, \tag{13}$$

where m is the thickness of aquifer. Equations for velocity components inside the circular intrusion according to eqs. (9) through (11) and (13) have the forms:

$$V_x = \frac{2\chi}{\chi+1}V_x^0, \ V_x^0 = \frac{Q}{2\pi m}\left(\frac{0.5d+x}{(0.5d+x)^2+y^2} + \frac{0.5d-x}{(0.5d-x)^2+y^2}\right)$$

$$Vy = \frac{2\chi}{\chi+1}V_y^0, \quad V_x^0 = \frac{Q}{2\pi m}\left(\frac{y}{(0.5d+x)^2+y^2} - \frac{y}{(0.5d-x)^2+y^2}\right). \tag{14}$$

Outside the inclusion they have the forms:

$$V_x = V_x^o + v_x'\cos\varphi_i - v_y'\sin\varphi_i - v_x''\cos\varphi_w + v_y''\sin\varphi_w$$

$$V_y = V_y^o + v_y'\cos\varphi_i - v_x'\sin\varphi_i - v_y''\cos\varphi_w - v_x''\sin\varphi_w, \tag{15}$$

where

$$v_x' = \frac{Q}{2\pi T_2}\frac{\chi-1}{\chi+1}\frac{x'-\beta_i R}{x'^2+y'^2}, \quad v_y' = \frac{Q}{2\pi T_2}\frac{\chi-1}{\chi+1}\frac{y'}{x'^2+y'^2}, \tag{15a}$$

and the coordinates x', y' are calculated according to eq. (11a). Equations for v_x'', v_y'' have the same structure as eq. (15a), where coordinates x', y' are changed to x'' and y'', and β_i to β_w.

The system of equations (12) with the initial condition of determined coordinates for particles was integrated in dimensionless form using the fourth-order explicit Runge-Kutta algorithm. For greater accuracy the time step Δt of integration is chosen so that the maximum displacement of the particle is no more than the small Courant number Co, i.e.,

$$\frac{\sqrt{V_x^2+V_y^2}}{n}\Delta t \le Co. \tag{16}$$

The particle is collected when it reaches the small area with radius R_{end} surrounding the pumping well, and the particle is recorded as having arrived at the well. At the time of the particle arrival at the pumping well, the withdrawal tracer concentration is calculated as k/N, where k is the number of particles arrived at the pumping well up to that time and N is the total number of injected particles. To test this algorithm, numerical results are compared with the analytical solutions for the breakthrough curve in the homogeneous aquifer (See Appendix B). It was found that by using the Courant number equal to 0.001

of the doublet dimension, d; the total number of particles equal to 1000, and $R_{int} = R_{end}$ equal to 0.001 of the doublet dimension, the difference between the numerical and analytical solutions is less than 1%. Coordinates of particles during the tracking procedures are used to draw the flow streamlines. Figure 2 shows an example of streamlines for the case of a circular inclusion with permeability higher than that of the surroundings.

RESULTS

Let us consider the results of a pumping test in this system. The average value of transmissivity T_{av} for this test is calculated by substituting the drawdown of groundwater head, S, at a point r_i and r_w from the injection and withdrawal wells respectively, into the solution for a doublet test in a homogeneous aquifer (*Desbarats*, 1993)

$$T_{av} = \frac{Q \ln \frac{r_w^2}{r_i^2}}{4\pi S} \tag{17}$$

On the other hand, according to eq. (9), the theoretical expression for transmissivity has the form

$$T_{av} = T_2 \frac{\ln \frac{r_w^2}{r_i^2}}{\ln \frac{r_w^2}{r_i^2} + S_i' + S_w'} . \tag{18}$$

It is easy to use eq. (18) to obtain values for the various locations of the inclusion and the point of observation. For example, if the center of inclusion is halfway between the wells, and the point of observation is inside the inclusion, the theoretical value of averaged transmissivity has the form

$$T_{av} = 2T_2 \frac{\chi+1}{\chi+3}. \tag{19}$$

It means that as the ratio of transmissivities inside and outside changes from zero to infinity, the average value varies from 2/3 to 2 times the aquifer transmissivity.

One can find from the structure of the equations (10) and (11) for the drawdown that the influence of the inclusion is determined by the distances from the wells to the center of the inclusion and the ratios of these distances to the radius of inclusion. So the most significant effect of the inclusion becomes visible when it is placed between the wells, i.e., the center of the inclusion lies at the origin of the coordinate system and the radius of the inclusion assumed to be equal to half the distance between the wells (Figure 3). Thus the influence of the inclusion was studied for this particular geometry and several sets of calculations were performed. The results are discussed below.

The first set assumes the same porosity inside as outside of the inclusion, and the calculations explore different ratios of transmissivities χ from zero for case of the impermeable inclusion to infinity for the case of the highly permeable inclusion. Tracer arrival times to the pumping well are used to estimate aquifer porosity (Appendix B). For cases when the transmissivity of the inclusion is equal to or more than the transmissivity of the aquifer, the relationship between the arrival time and the aquifer parameters can be found by integrating along the streamline $y(x) = 0$:

$$t_0 = n_1 \int_{-0.5d}^{0.5d} \frac{dx}{V_x} = \frac{(\chi+1)n_1\pi d^2 m}{6Q\chi} \tag{20}$$

or,

$$\tau = \frac{t_0 Q}{n_1\pi d^2 m} = \frac{1}{3}\,\frac{\chi+1}{2\chi} \tag{20a}$$

where τ is the dimensionless characteristic time for the doublet test in a uniform aquifer (see Appendix B). Here n_1 is the porosity of the inclusion, noting that the fastest flow path between the injection and production wells resides entirely in the inclusion. Equations (20) and (20a) show that increasing the transmissivity of the inclusion from a value equal to that of the aquifer to a very large value decreases the arrival time only by a factor of 2. So using analytical solution of arrival time for uniform aquifer to calculate porosity will yield an estimated value less than the real one and the maximum error should be less than 100%.

For cases where the transmissivity of the inclusion is less than the transmissivity of the aquifer, the earliest tracer arrival to the pumping well do not follow the streamline $y(x) = 0$, and eq. (20) would give the wrong arrival time. In Fig. 4 are shown results of the numerical calculations of the earliest tracer arrival time for a wide range of χ values. According to Fig. 4, the relationship between the arrival time and the ratio of transmissivities has non-monotonous shape with the maximum earliest arrival time equal to $0.667\,\tau$ at χ equal approximately to 0.3. It means that for the case of a low permeable inclusion, the maximum error for porosity estimated by means of tracer arrival time is also less than 100%. When the radius of the inclusion decreases or the distances between the inclusion and the wells increase, this error dramatically decreases. The shapes of the plume body for different ratios of transmissivities are shown in Fig. 3 for the case where the inclusion is between the two wells with its diameter equal to the distance between the wells. One can see from Fig. 3 that for a relatively small permeability of the inclusion ($\chi = 0.5$), the shape of plume body has a complex form with a pair of "toes" at the boundary of the inclusion. This complex plume body depends on the complexity of the field of velocity and gives breakthrough curves that do not at all look like the curves for the uniform aquifer (Fig. 5). It is noted that for relatively large values of time, the differences between the curves is not decreasing, so that their shapes are not of sufficient contrast for the prediction of the inclusion's parameters. This means that extending the test to large time periods would not give additional information about the aquifer parameters.

The second set of calculations of the breakthrough curves demonstrate the influence of changing the porosity when a highly permeable inclusion is placed between the wells. The results of these calculations are shown in Fig. 6. The numerically calculated tracer arrival time agrees well with the value predicted by eq. (20a). The tracer arrival time for the same porosity inside and outside the inclusion (the curve marked by number 1) is about 0.167, corresponding to the result of eq. (20a) with $\chi = \infty$. It is two times less than the tracer arrival time for the uniform aquifer. The tracer arrival time proportionally increases

with porosity as predicted by eq. (20). For the ratio of porosity equals to 5, the tracer arrival time is about 0.84, for ratio equals 10 this time is 1.67 and so on. Thus the porosity estimated by eq. (B2) for a homogeneous aquifer using the tracer arrival time can be quite wrong. For example in the case the same porosity inside and outside the inclusion, the tracer arrival time is two times smaller, which means that the estimated porosity will be two times less than the real porosity of aquifer. The theoretical value of effective porosity $\bar{n}$ estimated by tracer arrival time can be found by combining eq. (20a) and (B2):

$$\frac{\bar{n}}{n_2} = \frac{n_1}{n_2} \frac{\chi_1+1}{2\chi_1} \tag{21}$$

where n_2 is the porosity of the medium (outside of the inclusion). One can see from this equation that the estimated value of porosity depends on the ratio of transmissivities as well as the ratio of porosity, but the latter ratio influences the calculated result much more. Thus the effectively porosity $\bar{n}$ estimated by using the arrival time (eq. (21)) for highly permeable inclusion will be approximately half of the value in the inclusion and is not dependent on the porosity value in the other part of the aquifer.

The last set of calculations deals with the influence of the inclusion's location relative to the doublet wells. An impermeable inclusion, whose diameter is the same as the distance between the wells, is located at different distances from the origin of the coordinates for the purpose of studying the influence of the location on the shape of the breakthrough curves. The results of these calculations for the inclusion centered at the points with a constant x_c coordinate equal to 0 and three coordinates of y_c equal to 0, 0.5, and 1 of the distance between the wells are shown in Fig. 7. It is clear from this figure that as the inclusion is removed from the center of the doublet system at a distance approximately equal to the doublet dimension, it does not significantly influence the results of the tracer tests. Also, for smaller distances the influence is complex; for example, the arrival time could be less as well as more than the theoretical value calculated for a uniform aquifer.

CONCLUSIONS

The simple model of aquifer heterogeneity in the form of a circular inclusion with transmissivity different from that of the aquifer was studied in this paper. The choice of this model allows us to estimate the influence of the heterogeneity on flow and transport as a function of aquifer parameters inside and outside the zone of heterogeneity and also as a function of the ratio of its dimension to the dimension of the doublet system.

Precise numerical calculations of breakthrough curves using explicit analytical equations for the velocity fields showed complex results. One can find these breakthrough curves in Figures. 5, 6, and 7. They are calculated for the case of continuous injection and have a non-monotonous slope with the points of discontinuous derivatives. It means that in terms of instaneous injection, the breakthrough curves would have multiple peaks as was found in the work of *Tsang and Moreno* (1991) for the stochastic model of aquifer heterogeneity with a large variation of permeability. This implies that the multiple peak pattern of field tracer breakthrough curves may be found for less strongly heterogeneous systems by placing the wells close to a relatively large zone of heterogeneity.

The early tracer arrival time (or the extracted volume of water with tracer concentration 0–0.3 of the injected value) is a good measure for estimating the aquifer's porosity for aquifers which have non-constant permeability and relatively constant porosity. The theoretical error of the porosity value gotten by processing the test data using an analytical solution, according to our results, should not exceed 100%. It corresponds well with the results of stochastic modeling of tracer tests when the scale of transmissivity heterogeneity is equal to the doublet dimension (*Pozdniakov and Tsang*, 1994). This conclusion may be valid for some cases of porous media that do not have a strong correlation between porosity and permeability. As a rule, fractured media have positive correlation between porosity and permeability, and tracer arrival time for tests in such media can vary widely.

In general, changing the porosity has more influence on breakthrough curves than permeability. One can find from the structure of eq. (20) for the tracer arrival time that the porosity has a direct influence on time, whereas the effect of permeability change is in terms of a weaker function.

$$(\chi-1) / (\chi+1)$$

The size of the inclusion has a consequential effect on the breakthrough curves only if it is comparable to the doublet dimension. The tracer arrival time varies with the square of doublet dimension (Appendix B). One can find from Fig. 7 that, for an impermeable inclusion, tracer delay factor due to flow past an inclusion is approximately equals $\pi/2$. It means that the arrival time delay, or the effect of the inclusion, is proportional to $\pi R^2/d^2$ and quickly decreases as the size of the inclusion becomes much less than the doublet dimension.

ACKNOWLEDGMENTS

We appreciate the review and comments from Dr. Jahan Noorishad. The work was jointly supported by the Department of Energy, Office of Environmental Management, Office of Technology Development (DOE/EM-OTD) and the Department of Energy, Office of Energy Research, Office of Basic Energy Sciences (DOE/ER-BES), under Contract Number DE-AC03-76F00098.

REFERENCES

Butler, J.J. and Liu W. (1993), "Pumping Test in Nonuniform Aquifers: The Radially Asymmetric Case," *Water Resources Research*, 29, N2, 259–269.

Desbarats A.J. (1993), "Geostatistical Analysis of Interwell Transmissivity in Heterogeneous Aquifer," *Water Resources Research* 4, 1239–1246.

Golubeva, O.V. (1966), "Obobshenie teoremy ob okrugnosty na finltracionnye techenia," Isvestia AN SSSR, Mexanika gidkosti i gaza, N1, 113–116 (in Russian).

Herzog F. (1991), "A Simple Transport Model for the Grimsel Migration Experiments," PSI-Bericht, Nr. 106.

Huyakorn P.S., Andersen P.F., Guven O., and Moltz F.J. (1986), "A Curilinear Finite Element Model for Simulating Two Well Tracer Tests and Transport in Stratified Aquifers," *Water Resources Research*, 663.

Gradstein I.S. and Ryzhik M. (1965), *Table of Integrals, Series and Products*, New York, Academic Press.

Gelhar L.J. (1993), *Stochastic Subsurface Hydrology*, Prentice-Hall, Inc., New Jersey.

Gomez-Hernandez J.J. and Gorelick S.M. (1989), "Effective Ground Water Model Parameter Values: Influence of Spatial Variability of Hydraulic Conductivity, Leakance and Recharge," *Water Resources Research* 3, 405–419.

Grove D.V. (1971), *An Analysis of the Flow Field of a Discharging-Recharging Pair of Wells*, USGS Report 474-99, NTIS, 1971, 52 pp.

Grove D.V. and Beetem W.A. (1971), "Porosity and Dispersion Constant Calculations for a Tractured Carbonate Aquifer Using the Two-Well Tracer Methods," *Water Resources Research* 128–137.

Kurowski P., Ippolito I., Hulin J.P., Koplik J., and Hinch E.J. (1994), "Anomalous Dispersion in a Dipole Flow Geometry," *Physics of Fluids*, 1, 108–117.

Landau L.D. and Lifshitz E.M. (1962), *The Classical Theory of Fields*, Oxford Pergamon Press.

Mironenko V.A. and Rumynin V.G. (1986), *Optino Migracionnie Raboty v Vodonostnyx Plastax*, Nedra, Moscow.

Moreno L., and Tsang C.F., (1991), "Multiple-Peak Response to Tracer Injection Tests in Single Fractures: A Numerical Study," *Water Resources Research* 27, 2143–2150.

Pozdniakov S.P. and Tsang C.F. (1994), "Tracer Transport Modeling of the Doublet Well System," in *Numerical Methods in Water Resources*, Kluwer Academic Publishers.

Strack O.D.L. (1989), *Grondwater Mechanics*, Prentice-Hall, Inc.

Tsang Y.W., Tsang C.F., Neretnicks I., and Moreno L. (1988), "Flow and Tracer Transport in Fractured Media: A Variable Aperture Channel Model and Its Properties," *Water Resources Research* 12, 2049-2060.

APPENDIX A

Equations for flow toward a well near the circular inclusion in a polar system of coordinates.

It is to trivial to show that the continuous solution of eq. (4) within a circular inclusion has a general form ρ

$$U_1 = \sum_{k=0}^{\infty} a_k p^k \cos k\theta, \quad p = r/R_o < 1 . \tag{A.1}$$

Whereas field U_2 outside the circle for $r > R$ must be taken in the form

$$U_2 = b_0 \ln r + \sum_{k=1}^{\infty} b_k p^{-k} \cos\theta , \tag{A.1a}$$

where a_k and b_k are unknown coefficients.

To determine these coefficients, we must satisfy the boundary conditions. This can be done by putting the initial field eq. (2) in the form

$$U_0 = U^0 + \frac{Q}{2\pi T_2}\left(\ln\frac{R_0}{\Omega} - \sum_{k=1}^{\infty} \frac{p^k \cos k\theta}{k} \right). \tag{A.2}$$

where we have used the representation of a log in series (*Gradstein, Ryzhik*, 1965)

$$\ln\sqrt{1+p^2-2p\cos\theta} = -\sum_{k=1}^{\infty} \frac{p^k \cos k\theta}{k} , \tag{A.3}$$

Substituting eqs. (A.2), (A,1), and (A.1a) in the boundary conditions and using the orthogonal properties of $\cos k\theta$ we find for $k = 0$

$$b_0 = 0 \quad a_0 = U^0 + \frac{Q}{2\pi T_2} \ln\frac{R_0}{\Omega} . \tag{A.4}$$

For each values of $k > 0$, we get a system of two linear equations which have the solution

$$b_k = \frac{Q}{2\pi T_2}\frac{1-\chi}{1+\chi}\frac{s^k p^k}{k}, \quad \chi = \frac{T_1}{T_2}; \quad s = \frac{R^2}{R_0 r} \tag{A.5}$$

$$a_k = -\frac{Q}{2\pi T_2}\frac{2}{1+\chi}\frac{1}{k}. \tag{A.5a}$$

Using the log representaton of a series, i.e., eq. (A.3), finally we get the equations for the field in cylindric coordinates:

$$U_1 = U^0 + \frac{Q}{2\pi T_2}\left(\ln\frac{R_0}{\Omega} + \frac{2}{1+\chi}\ln\sqrt{1+p^2-2p\cos\theta}\right) = \mathrm{U}_o + \frac{\mathrm{Q}}{2\pi T_2}\frac{1-\chi}{1+\chi}\ln\frac{\rho}{R_o} \tag{A.6}$$

$$U_2 = -\frac{Q}{2\pi T_2}\frac{1-\chi}{1+\chi}\ln\sqrt{1+s^2-2s\cos\theta}. \tag{A.6a}$$

When a hydraulic head

$$U_o = U^o + \frac{Q}{2\pi T_1}\ln\frac{\rho}{\Omega} \tag{A.7}$$

is applied inside of the inclusion, the way of obtaining the solution is quite analogous. The hydraulic head (A.7) induces additional fields, U_1 and U_2, inside and outside the inclusion respectively, given by

$$U_1 = \frac{Q}{2\pi T_1}\frac{1-\chi}{1+\chi}\ln\frac{\rho}{R_o} \tag{A.8}$$

$$U_2 = U_o\frac{Q}{2\pi T_1}\frac{1-\chi}{1+\chi}\ln\sqrt{1+s^2-2s\cos\theta}. \tag{A.9}$$

APPENDIX B

Breakthrough curve for doublet well test with a continuous tracer injection

In this section we outline a method for obtaining the breakthrough tracer curve in the pumping well during a doublet-well tracer test. According to the solution obtained by *Mironenko and Rumynin* (1986), the dimensionless concentration C in the pumping well is given by

$$C(\tau) = \pi^{-1}\inf F(\psi),\ \ \tau = \frac{tQ}{\pi d^2 nm},\ \ F(\psi) = \frac{\sin\psi - \psi\cos\psi}{\sin^{3\psi}} = r\ , \tag{B.1}$$

where inf F is the function inverse to F.

Here, $C = 0$ for time $\tau < \tau_0 = 1/3$, $C > 0$ for $\tau > \tau_0$ (Fig. 8), and $C = 0.5$ for time $\tau = 1$, which enables one to use the onset time of tracer arrival (t_0) or time for $C = 0.5(t_{0.5})$ as interpretation parameters

$$n = \frac{3t_0 Q}{\pi d^2 m} \text{ or } \frac{t_{0.5} Q}{\pi d^2 m}\ . \tag{B.2}$$

An approximation of the solution eq. (B.1) for small concentration values can be obtained using a series representation of sin and cos for a small number of angles. An approximation solution for dimensionless concentration (concentration less than 0.25–0.3) has the form

$$C = \frac{1}{\pi}\sqrt{\frac{3\tau - 1}{1.5\tau - 0.1}}\ . \tag{B.3}$$

For relatively large concentrations ($C > 0.5$ to 0.6), the well approximation of solution eq. (B.1) is the solution for a perfect dipole obtained by *Kurowski et al.* (1994) in the form

$$C = 1 - \frac{2}{3}\frac{k}{\pi^3\sqrt{\tau}}\ ,\ \ k \approx 2.1\ . \tag{B.4}$$

Breakthrough curves calculated according to eqs. (B.1), (B.3), and (B.4) are shown in Fig. 8.

APPENDIX C

Field of an equal dipole near a circular inclusion

In this section, we outline a method for obtaining the solution for an equal dipole near a circular inclusion based on the general solution for a source near the inclusion (Appendix A). When the distance l between sink and source with all equal flow rate Q is small, and the solution for the doublet can be obtained from the solution of a perfect dipole (*Kurowski et al.*, 1994). The equivalent perfect dipole has a moment equal to Ql, and its field can be calculated as

$$U_d = l\frac{dU}{dl}, \tag{C.1}$$

where U is the field of the single sink/source and U_d is the field of the perfect dipole.

Let us assume that for the configuration shown in Fig. 1 the perfect dipole ($l \sim o$) is placed on axis X distance R_0 from the center of the inclusion, and it is angle α to the X axis. The field of the dipole can then be calculated through eqs. (A11a) and (A11b) using the standard rule

$$U_d = l\left(\frac{\partial U}{\partial R_0}\frac{\partial R_0}{dl} + \frac{\partial U}{\partial \theta}\frac{d\theta}{dl}\right), \tag{C.2}$$

where

$$\frac{d\theta}{dl} = -\frac{\sin\alpha}{R_0}\frac{dR_0}{dl} = \cos\alpha\ . \tag{C.3}$$

FIGURE CAPTIONS

Fig. 1. Geometry of the problem of a source placed near the inclusion.

Fig. 2. Geometry of the problem and flow lines for the case of a circular inclusion with permeability higher than that of the surroundings.

Fig. 3. The perticular case where the circular inclusion is assumed to fill the area between the injection and pumping wells. The shapes of the injected liquid

plume body at the time of the tracer arrival at the pumping well are shown for different χ values, 0.5, 1, and 100.

Fig. 4. Relationship between the earliest tracer arrival time and the ratio of transmissivities.

Fig. 5. Breakthrough curves for various values of χ from 0 to 100.

Fig. 6. Breakthrough curves for the case of a highly permeable inclusion. The curves are labelled by numbers, giving the ratio of the porosity of the inclusion and the porosity of the surrounding rock.

Fig. 7. Breakthrough curves for different distances between the inclusion and the doublet center. The curves are labelled by numbers, giving the dimensionless distances between the inclusion and the doublet center.

Fig. 8. Theoretical breakthrough curve for a doublet well system.

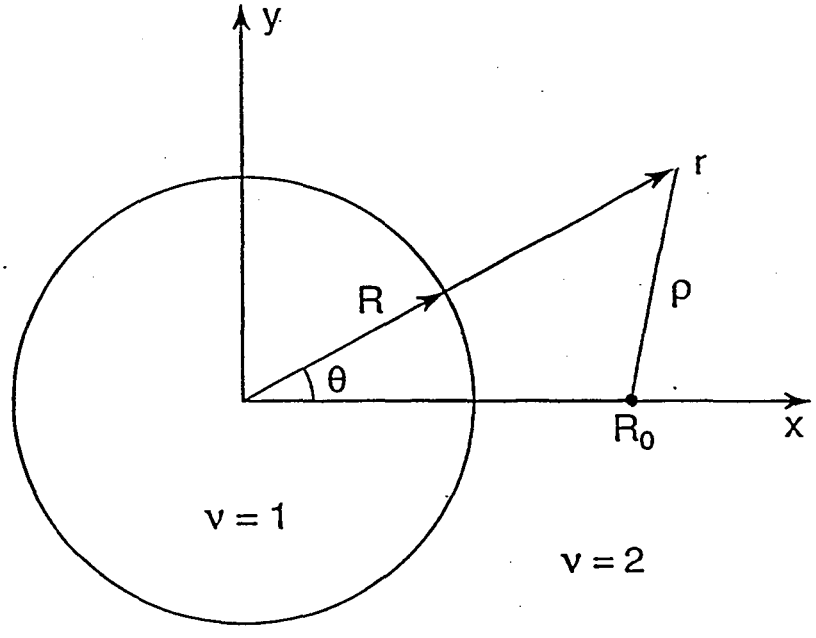

XBD 9507-03369.ILR

Figure 1.

Flow lines for case of highly permeable inclusion

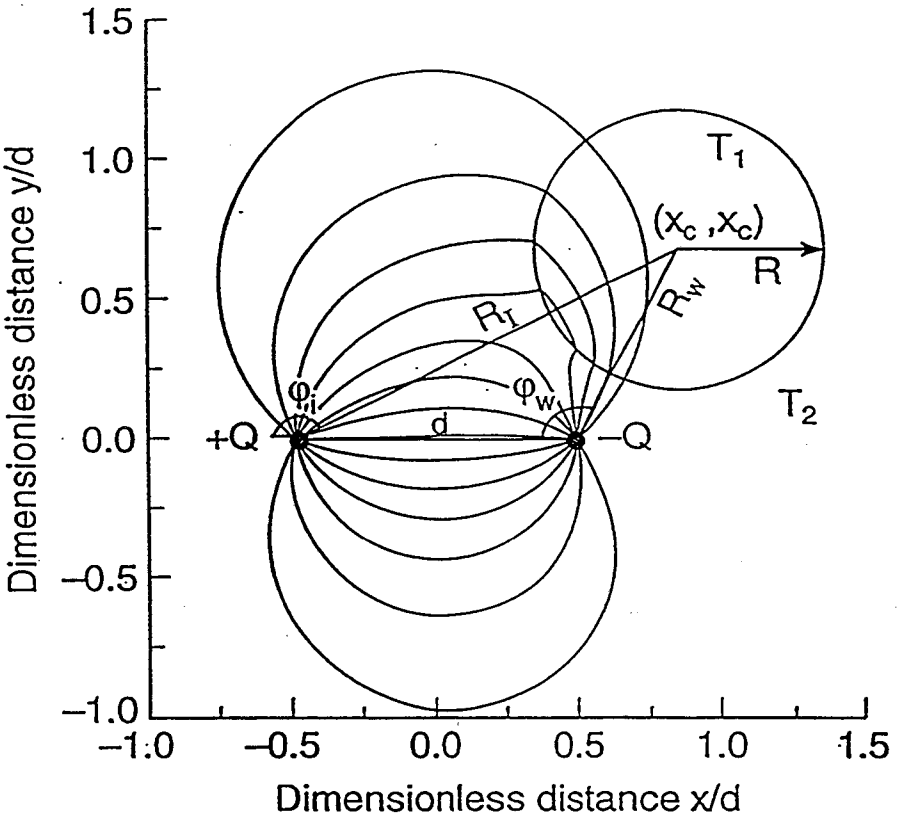

XBD 9507-03370.ILR

Figure 2.

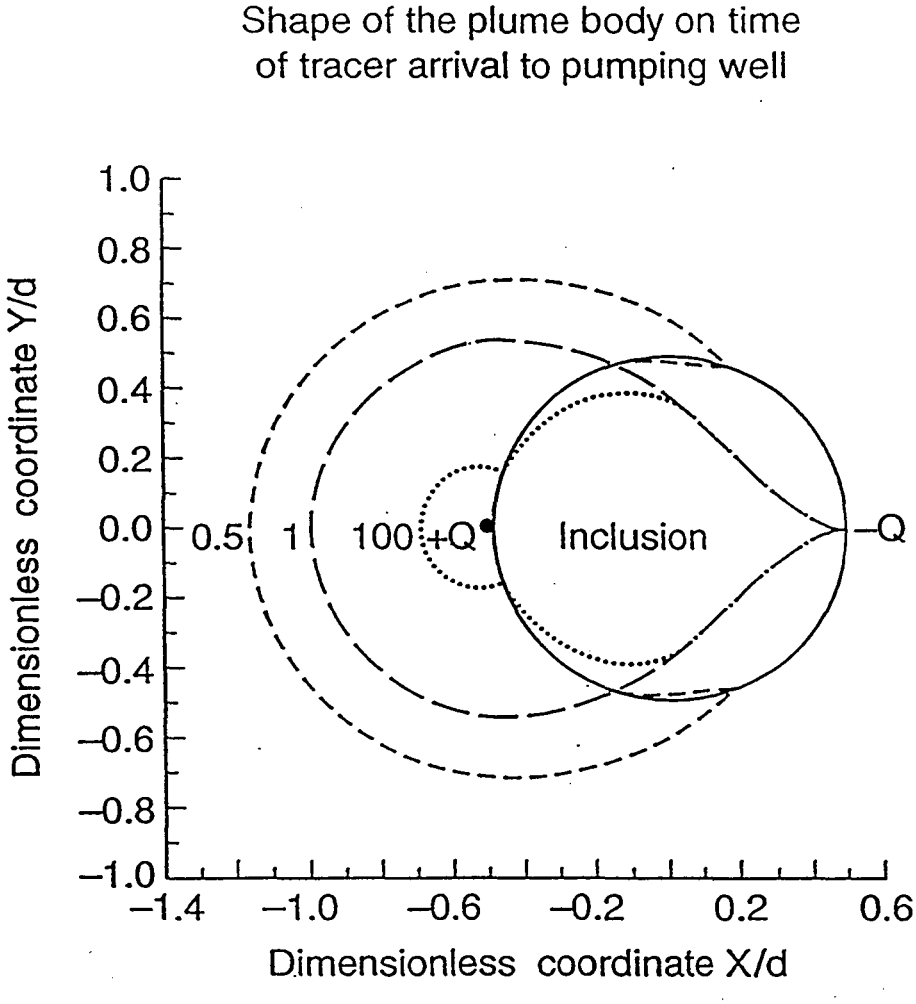

Figure 3.

XBD 9507-03372.ILR

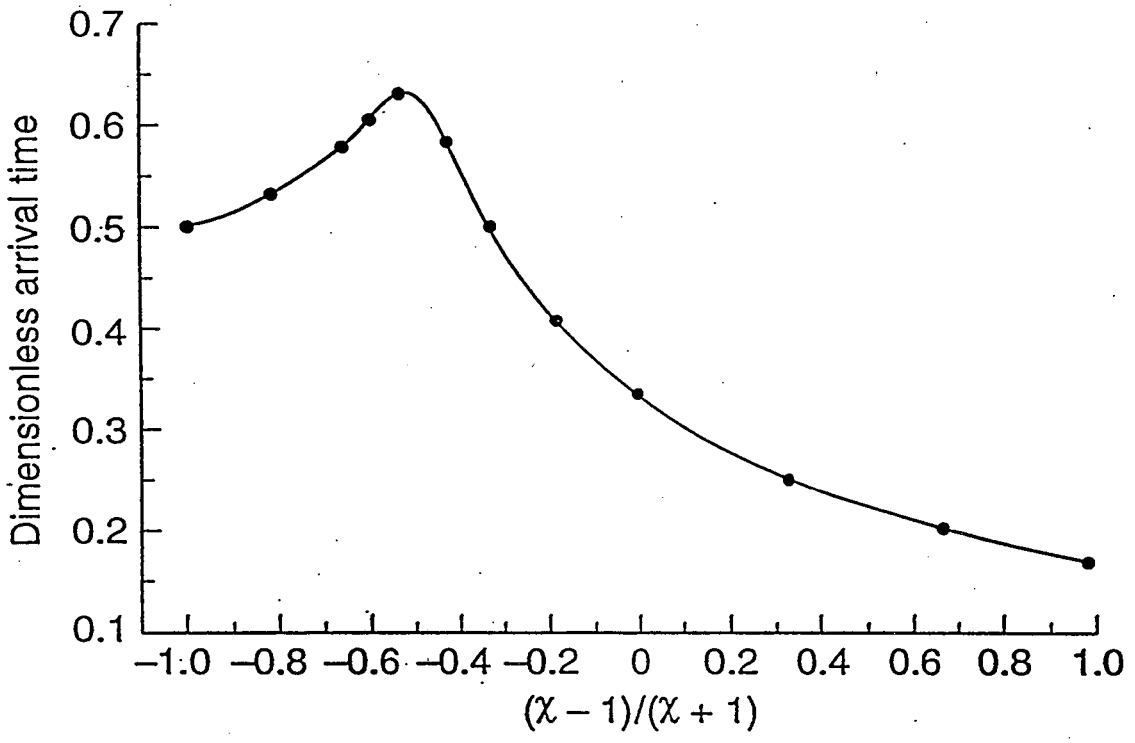

Figure 4.

XBD 9507-03371.ILR

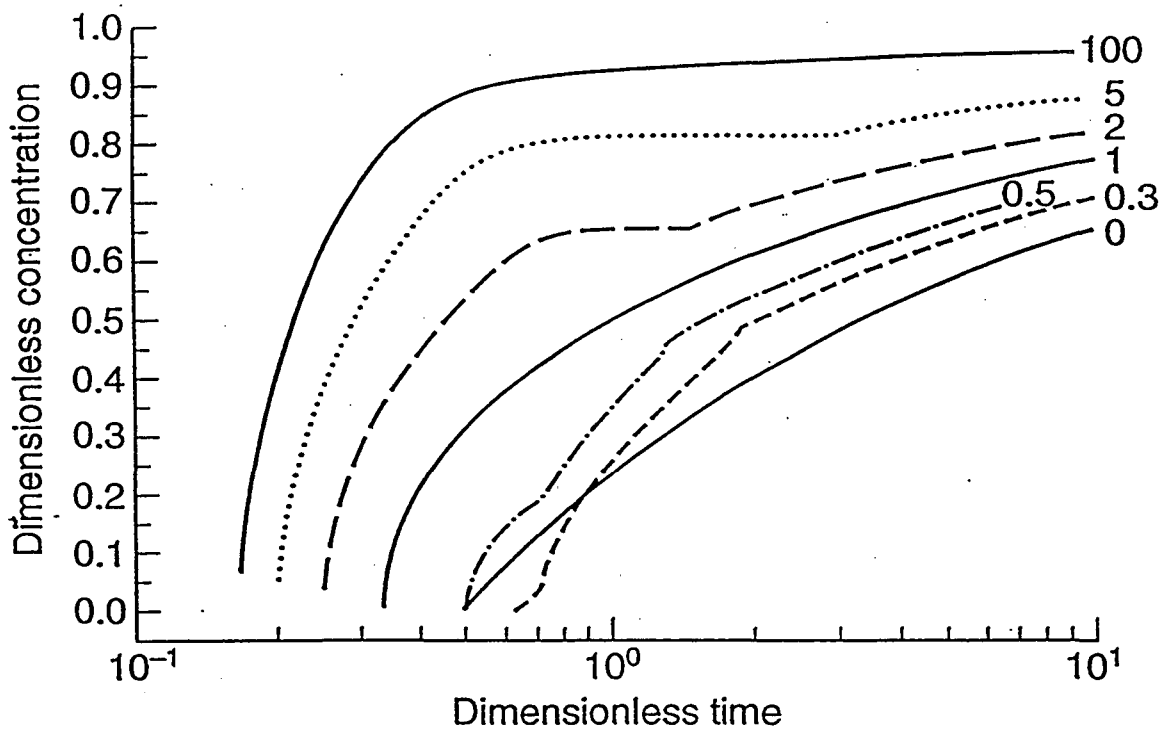

XBD 9507-03373.ILR

Figure 5.

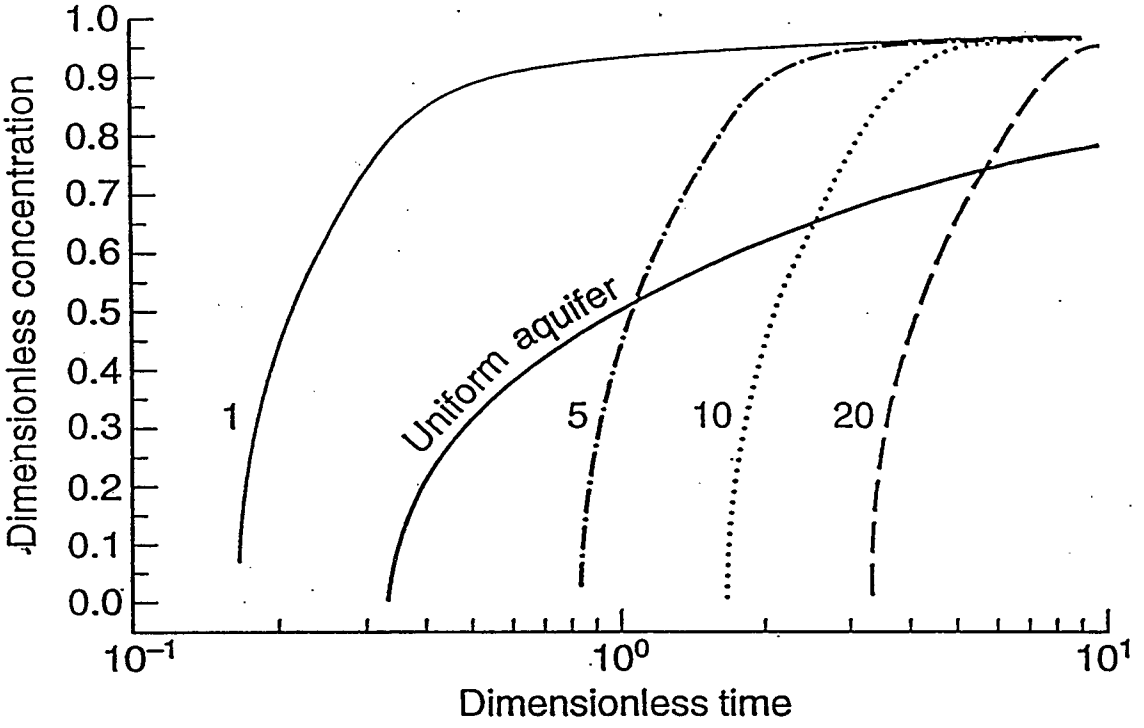

XBD 9507-03374.ILR

Figure 6.

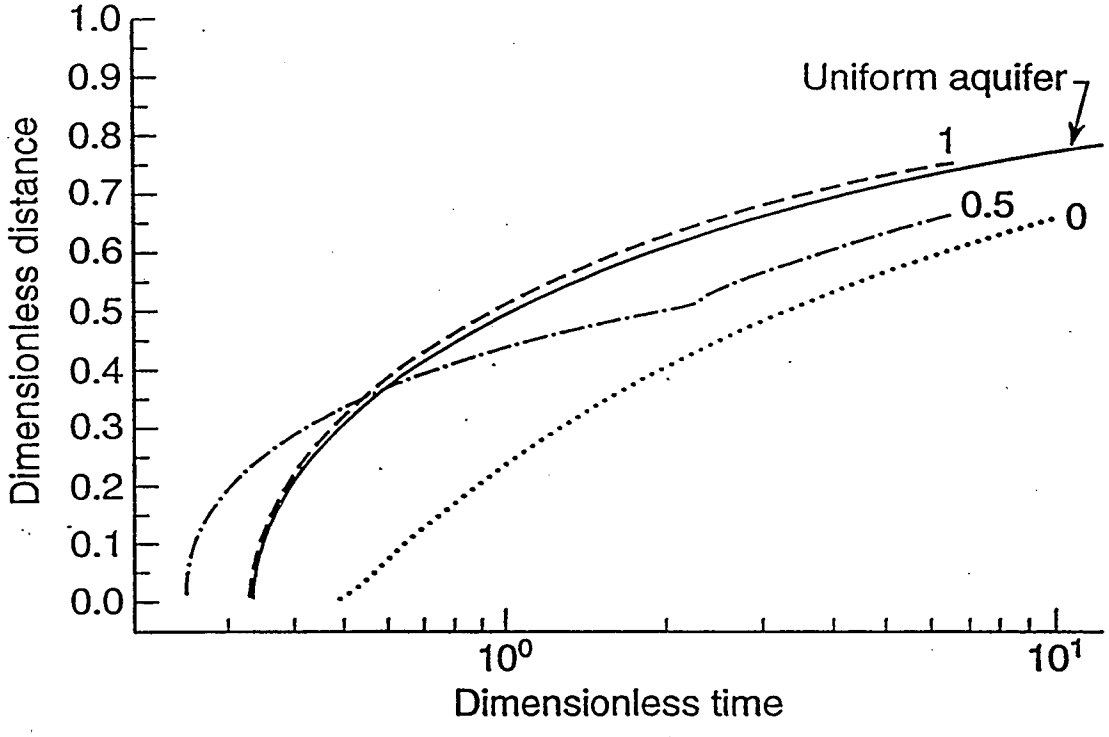

XBD 9507-03375.ILR

Figure 7.

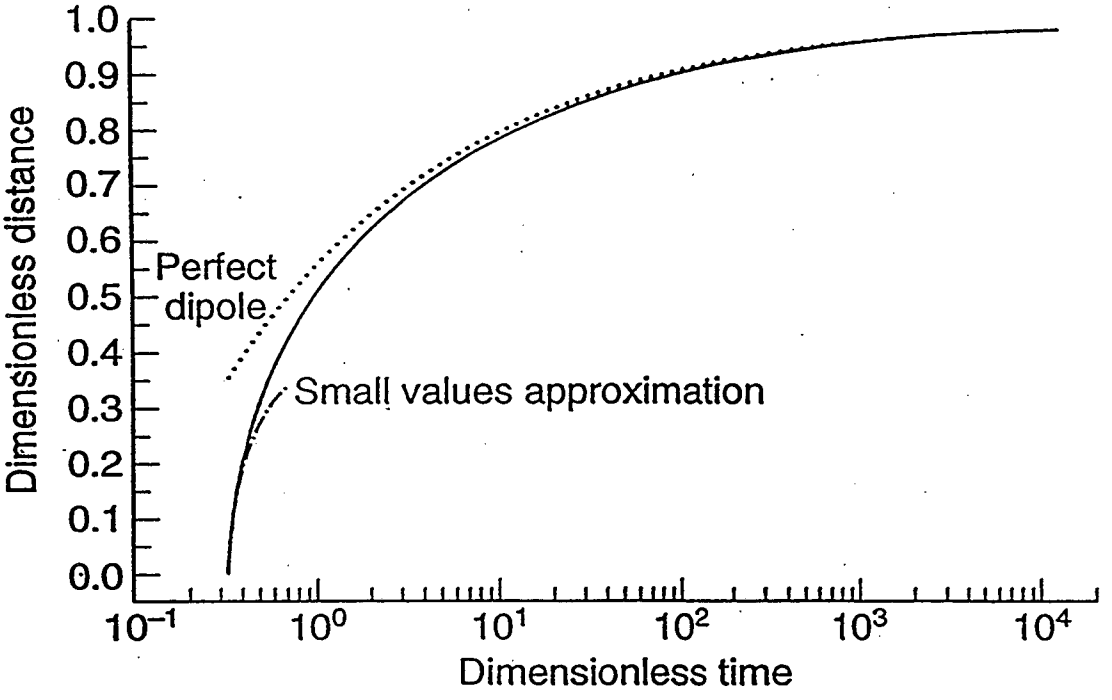

XBD 9507-03376.ILR

Figure 8.

LAWRENCE BERKELEY NATIONAL LABORATORY
UNIVERSITY OF CALIFORNIA
TECHNICAL & ELECTRONIC INFORMATION DEPARTMENT
BERKELEY, CALIFORNIA 94720